Ultrasensitive Silicon Nanowire for Real-World Gas Sensing: Noninvasive Diagnosis of Cancer from Breath Volatolome

ARTICLE *in* NANO LETTERS · DECEMBER 2014

Impact Factor: 13.59 · DOI: 10.1021/nl504482t · Source: PubMed

6 AUTHORS, INCLUDING:

Konrads Funka
University of Latvia
17 PUBLICATIONS **112** CITATIONS
SEE PROFILE

Silke Christiansen
Helmholtz-Zentrum Berlin
311 PUBLICATIONS **4,422** CITATIONS
SEE PROFILE

Hossam Haick
Technion - Israel Institute of Technology
158 PUBLICATIONS **4,439** CITATIONS
SEE PROFILE

NANO LETTERS

Letter

pubs.acs.org/NanoLett

Ultrasensitive Silicon Nanowire for Real-World Gas Sensing: Noninvasive Diagnosis of Cancer from Breath Volatolome

Nisreen Shehada,[†] Gerald Brönstrup,[‡] Konrads Funka,[§,∥,⊥] Silke Christiansen,[‡] Marcis Leja,[§,∥,⊥] and Hossam Haick*,[†]

[†]The Department of Chemical Engineering and Russell Berrie Nanotechnology Institute, Technion—Israel Institute of Technology, Haifa 3200003, Israel

[‡]Max-Planck-Institute for the Science of Light, Günther-Scharowsky-Strasse 1, 91058 Erlangen, Germany

[§]Faculty of Medicine, University of Latvia, LV1006 Riga, Latvia

[∥]Department of Research, Riga East University Hospital, LV1006 Riga, Latvia

[⊥]Digestive Diseases Centre GASTRO, LV1006 Riga, Latvia

Supporting Information

ABSTRACT: We report on an ultrasensitive, molecularly modified silicon nanowire field effect transistor that brings together the lock-and-key and cross-reactive sensing worlds for the diagnosis of (gastric) cancer from exhaled volatolome. The sensor is able to selectively detect volatile organic compounds (VOCs) that are linked with gastric cancer conditions in exhaled breath and to discriminate them from environmental VOCs that exist in exhaled breath samples but do not relate to the gastric cancer per se. Using breath samples collected from actual patients with gastric cancer and from volunteers who do not have cancer, blind analysis validated the ability of the reported sensor to discriminate between gastric cancer and control conditions with >85% accuracy, irrespective of important confounding factors such as tobacco consumption and gender. The reported sensing approach paves the way to use the power of silicon nanowires for simple, inexpensive, portable, and noninvasive diagnosis of cancer and other disease conditions.

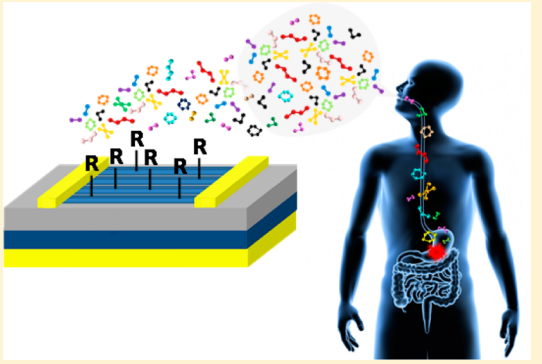

KEYWORDS: *Silicon nanowire, field effect transistor, cancer volatolomic, breath, diagnosis*

Cancer is a devastating disease accompanied by several medical challenges including delayed diagnosis, low efficacy of the anticancer therapy, and heterogeneity of the disease.[1] There is an urgent unmet need for inexpensive and noninvasive technology that would enable efficient early detection of cancer, stratifying the population based on biospecification for a tailored (personalized) therapy, and fast, bed-side assessment of treatment efficacy in order to change the therapeutic approach accordingly.[2] A promising approach to meet these challenges is based on the so-called volatolomics, namely, volatile organic compounds (VOCs) emanating from the cancer cells as well from their microenvironment.[3−8] These VOCs can be identified from the headspace of cancer cells lines (i.e., the blend of VOCs confined above the cells in a sealed flask),[9,10] through the urine, through the skin, through the blood, and/or through the exhaled breath.[4,11] The VOCs in these body fluids emerge at very early stages of the cancer so their isolation and detection could serve as a pathway for early detection of the cancer.[7,12] Of these body fluids, exhaled breath is one of the most useful VOC sources for monitoring body chemistry or state of health, because it can be obtained noninvasively, it is suitable for high compliance, and it provides a matrix of relatively low complexity.[3−8,13]

For breath volatolomic testing to become a clinical reality, several advances in the sensor development must occur (cf. refs 4 and 6, and citations therein). From the reservoir of available materials, sensor-based on silicon nanowires[14−22] are most promising, because they are significantly smaller, easier-to-use, and less expensive.[18−21,23−26] An ideal silicon nanowire chemical sensor for breath volatolome should be sensitive at very low VOC concentrations. Furthermore, it should respond rapidly and differently to small changes in concentration and provide a consistent output that is specific to a given exposure. When not in contact with the VOC, the sensor should return to its baseline state rapidly and be simple and inexpensive enough to manufacture large numbers of disposable units.

Two main sensing approaches have been tried recently to answer the aforementioned requirements for cancer diagnosis via breath volatolomics.[3,4,6] The first approach relies on selective detection of single compound(s), via, for instance, lock-and-key recognition.[26] Although this approach has allowed low-detection limits (down to a few ppbs) and high sensitivities toward ethanol[27] and other polar VOCs (e.g., N_2O, NO,

Received: November 22, 2014

   dx.doi.org/10.1021/nl504482t | *Nano Lett.* XXXX, XXX, XXX−XXX

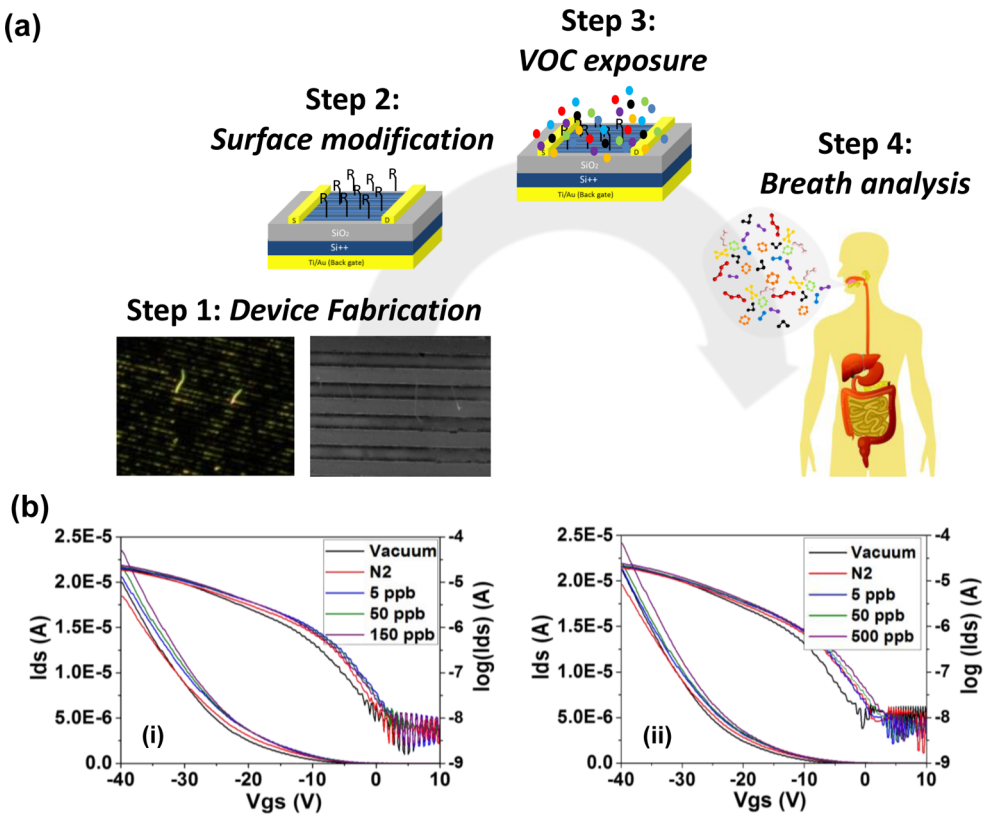

Figure 1. (a) Schematics demonstrating the main steps implemented in the present study: fabrication of SiNW FETs (step 1); modification of the SiNWs with molecular layers (step 2); exposure of the molecularly modified SiNW FETs to VOCs that are linked with gastric cancer conditions, and for comparison, to VOCs that serve as confounding environmental factors (step 3);[7] and exposure of the molecularly modified SiNW FETs to real breath samples collected from volunteers who have gastric cancer or from volunteers with control (healthy) conditions (step 4). (b) Representative example of source-drain current (I_{ds}) vs back-gate voltage (V_{gs}) curves of S1 in vacuum, upon exposure to N_2 and upon exposure for increasing concentrations of (i) VOC2 and (ii) VOC5.

Table 1. List of the Molecular Modifications Used in the Present Study To Impart Selectivity to the SiNW FETs towards the Gastric Cancer VOCs in Lab and Real-World (Clinical) Settings

Sensor no.	Modification	Structure
S1	Trichloro(phenethyl)silane (TPS)	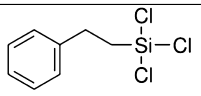
S2	Trichloro(3,3,3-trifluoropropyl) silane (TTPS)	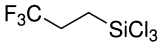
S3	Bare	SiO_2
S4	Propyl-Gallate	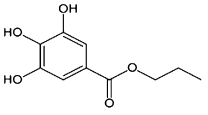
S5	Heptanoyl Chloride	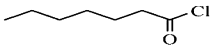
S6	Decanoyl Chloride	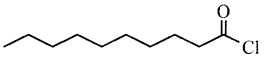
S7	3-Methyl-2-phenyl valeric acid	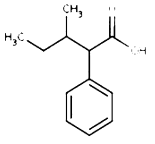

dx.doi.org/10.1021/nl504482t | Nano Lett. XXXX, XXX, XXX−XXX

Table 2. List of the VOCs Linked with Gastric Cancer from Exhaled Breath (VOC1−3)[a]

Name	Compound	Concentrations in experiment (ppb)	Concentrations in breath (ppb)	Structure
VOC1	2-Propenenitrile	50– 150	1.9 – 16.7	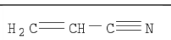
VOC2	6-Methyl-5-Hepten-2-one	5 – 150	16.3 – 37.6	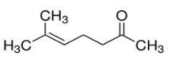
VOC3	Furfural (Furfuraldehyde)	5 – 500	2.5 – 10.3	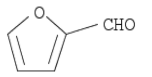
VOC4	2-Ethyl-1-hexanol	5 – 500	105.0 – 462.6	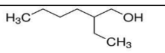
VOC5	Nonanal	5 – 500	57.2 – 179.1	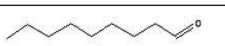

[a]A significant $\pm p < 0.05$ statistical difference is shown as well as confounding environmental factors that exist in the exhaled breath but do not relate to cancer (VOC4−5). The concentrations of the VOCs of interest in real exhaled breath of gastric cancer (based on mass spectromerty studies) as well as the concntrations range examined in the lab setting are listed.

CO),[26,28] success has not yet been achieved regarding the breath volatolomics of cancer. This lack of success can be attributed to the absence of biomarkers that appear solely in cancer states, compared to healthy (or control) states. Rather, the VOCs that characterize the cancer are found also in healthy human breath but in statistically distinctive mixture compositions.[3−6] An additional reason is the difficulty to synthesize selective receptors for the low molecular weight VOCs found in the exhaled breath of cancer states.[4,6]

The second approach relies on cross-reactive sensor arrays that impart different affinity from various combinations of gaseous species and achieve the required selectivity through sophisticated pattern recognition algorithms.[29] This approach has been successfully demonstrated for the detection of a wide variety of diseases, including cancer (cf. ref 8 and citations therein). Nevertheless, the dependence of this approach on the use of multiple sensors requires complicated circuitry and hardware, such as switches and multiplexers, as well as strong computation power to host the pattern recognition analysis of the wide variety of the output sensing signals.[29,30]

In this paper, we propose an intermediate approach that marries the selectivity of the lock-and-key approach to the ability to tailor the cross-reactive sensor arrays for complex fluids. The proposed approach is based on an individual molecularly modified silicon nanowire field effect transistor (SiNW FET) that supplies an assortment of independent features,[30−32] each of which responds differently to the various VOCs at the low part-per-billion (ppb) concentration level. On the other hand, the collective output of these features can be treated via simple pattern recognition methods to enable recognition of complicated mixtures. Ultimately, this approach requires simple hardware, as it is based on a single sensor, thus improving the ability to miniaturize the device and simplifying its use and facilitating its integration in pre-existing, silicon-based technologies. The capabilities of this approach/sensor are examined for the diagnosis of gastric cancer volatolome from real breath samples, collected from 107 volunteers with either gastric cancer or control conditions (see Figure 1a).

A molecularly modified SiNW FET coated with trichloro-(phenethyl)silane (TPS) was prepared for highly sensitive detection of gastric cancer VOCs both in lab and real-world clinical settings. In the current paper, we label this sensor as S1 (see Table 1). For the sake of comparison, SiNW FETs coated with other molecular modifications were prepared. These modifications are labeled as S2−S7 in Table 1. These sensors were exposed to various concentrations of VOCs that were linked in our earlier studies, via mass spectrometry, to gastric cancer conditions in exhaled breath (VOC1−3) as well as to confounding environmental factors (VOC4 and VOC5), which might exist in the breath but do not relate to the disease per se.[7] The VOCs, their concentration in real breath samples, and the examined concentrations in the lab setting are summarized in Table 2. For detailed information about the preparation of the SiNWs, fabrication of the SiNW FETs, molecular modifications of the SiNW FETs, and on the surface characterization of the produced devices, please refer to the Supporting Information (SI), sections 1.1−1.5.

Electrical and sensing signals were collected for 15 min under vacuum, followed by 15 min of sample exposure (chamber closed with the gas sample inside), and followed by an additional 15 min under vacuum. Generally, the experiment included a cycle of N_2 exposure as a baseline, followed by 6−8 cycles of exposure to VOCs (3−4 various concentrations and two exposures to each concentration). Characteristic source−drain current (I_{ds}) vs back gate voltage (V_{gs}) curves of S1 was obtained and analyzed in order to examine its response to the gastric cancer VOCs and to the confounding VOCs. More details about the exposure procedure of the SiNW FETs to the VOCs of interest are found in the SI, section 1.6.

Figure 1b presents the I_{ds} vs V_{gs} curves of S1 on exposure to VOC2 (Figure 1b-i) and VOC5 (Figure 1b-ii), in both linear (left Y-axis) and logarithmic (right Y-axis) scales. As seen in the figure, S1 responds to extremely low concentrations of VOC2 (down to 5 ppb). Indeed, the curve obtained on exposure to 5 ppb VOC2 (Figure 1b-i, blue line) can easily be differentiated from the curve corresponding to exposure to N_2 (Figure 1b-i, red line) or vacuum (Figure 1b-i, black line). In addition, the curves corresponding to different concentrations (5, 50, and 150 ppb) can be easily differentiated from one another. In contrast, the same sensor (S1) showed no differences between the responses to vacuum and various concentrations (5 and 50 ppb) of VOC5. These results indicate that S1 is selective to VOC2 (biomarkers of gastric cancer from exhaled breath), but

dx.doi.org/10.1021/nl504482t | Nano Lett. XXXX, XXX, XXX−XXX

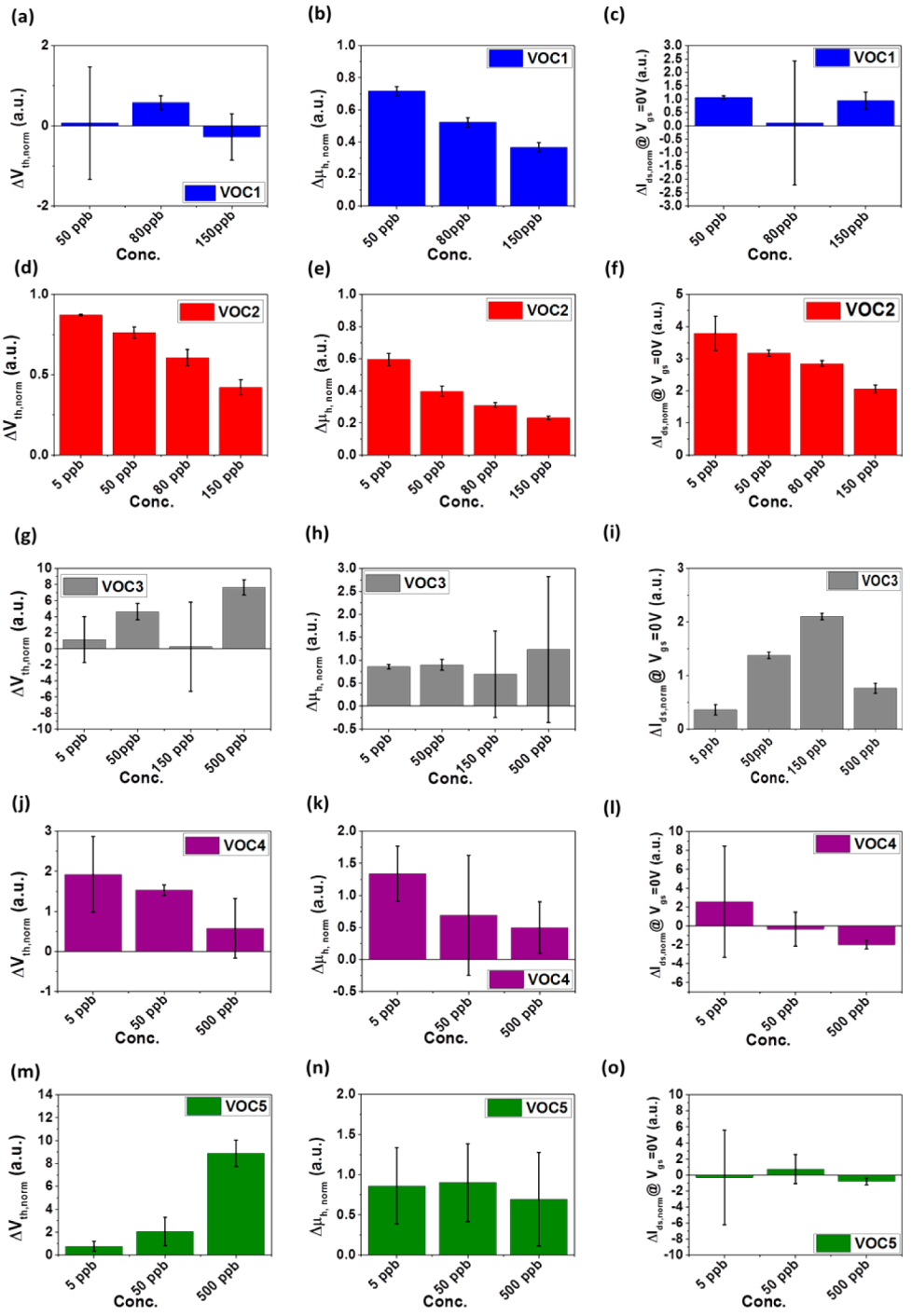

Figure 2. Response of the selected features ($\Delta V_{th,norm}$, $\Delta \mu_{h,norm}$, $\Delta I_{ds,norm}$ @ V_{gs} = 0) extracted from S1 in exposure to (a–c) VOC1, (d–f) VOC2, (g–i) VOC3, (j–l) VOC4, and to (m–o) VOC5. All values presented in this figure relate to the area-under-curve of the specific response during the exposure time of the specific VOC(s) normalized to the value of the area-under-curve during exposure to N_2.

not for VOC5 (confounding environmental VOC that does not relate to gastric cancer) in this range of concentrations.

A further examination of the sensing capabilities of S1 was achieved through extraction of three area-under-peak features from the characteristic I_{ds} vs V_{gs} curve: the threshold voltage (V_{th}); the charge carrier (hole) mobility (μ_h), extrapolated from the linear part of the curve; and the current at zero applied gate voltage (I_{ds} @ V_{gs} = 0), as a representative subthreshold current. All values presented here were compared to the vacuum level before the exposure cycle and then normalized to the value received in exposure to N_2, according to the following relationship:

$$R_{f,norm} = \frac{R_{f,VOC}}{R_{f,N_2}} = \frac{\int f_{VOC}\,dt}{\int f_{N_2}\,dt} = \frac{f_{VOC} - f_{vac}}{f_{N_2} - f_{vac}} = \frac{\Delta f_{VOC}}{\Delta f_{N_2}} \quad (1)$$

where $R_{f,norm}$ stands for the normalized response of the feature; $R_{f,VOC}$ is the response of the feature to a specific VOC; R_{f,N_2} is the response of the feature to nitrogen; f_{VOC} is the value of the

dx.doi.org/10.1021/nl504482t | Nano Lett. XXXX, XXX, XXX–XXX

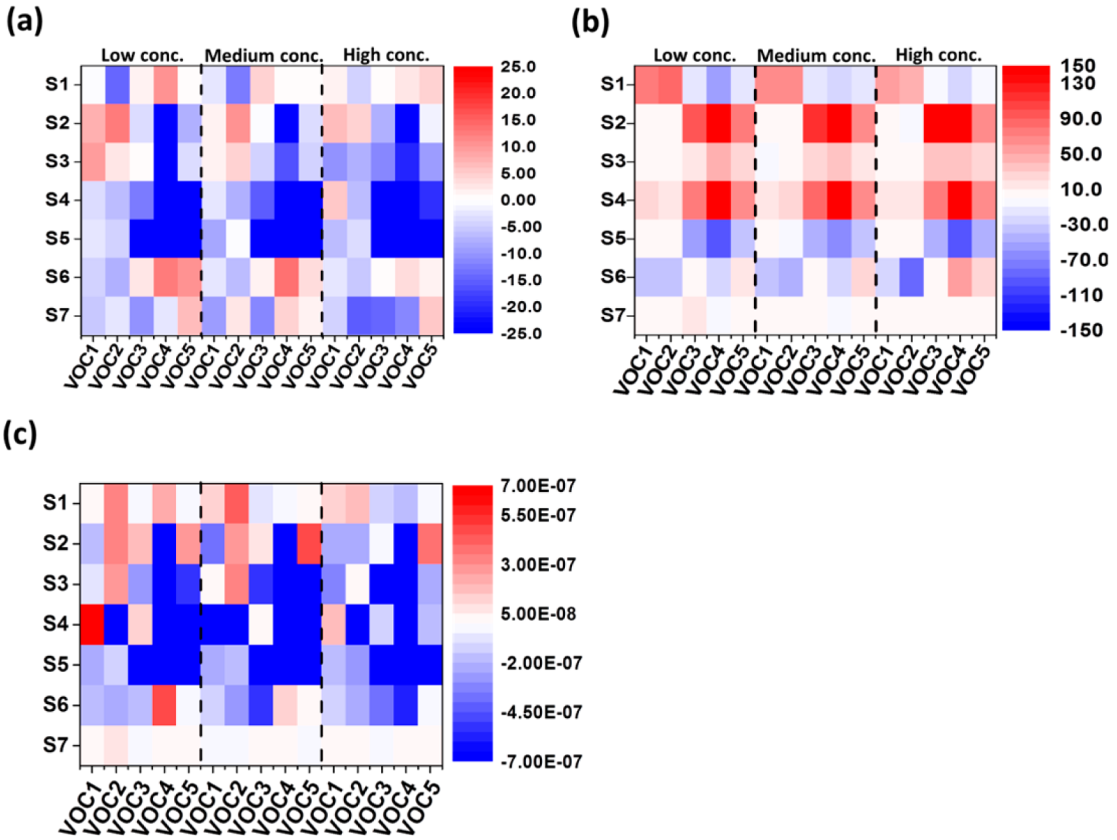

Figure 3. Hot plot of the average response of (a) V_{th}, (b) μ_h, and (c) I_{ds} @ V_{gs} = 0 of S1−S7 on exposure to various concentrations of VOC1 to VOC5. Low concentration stands for 5 ppb (50 ppb for VOC1); medium concentration stands for 50 ppb (80 ppb for VOC1); and high concentrations stand for 150−500 ppb.

feature under exposure to a specific VOC; f_{vac} is the value of the feature in vacuum; and f_{N_2} is the value of the feature under exposure to nitrogen (N_2). Examining the response of S1 to VOC1 shows that only the $\Delta\mu_{h,norm}$ is able to differentiate the various concentrations beyond the experimental error (Figure 2). In this case, there is a decrease in μ_h as a result of the exposure to increasing concentrations of the VOC, from a $\Delta\mu_{h,norm}$ value of 0.71 at 50 ppb VOC1, down to 0.37 at 150 ppb VOC1. Similar observations were obtained in the case of VOC2, where both $\Delta V_{th,norm}$ and $\Delta\mu_{h,norm}$ showed a significantly different response to increasing concentrations of the targeted VOCs. The response of $\Delta V_{th,norm}$ decreased from 0.87 when exposed to 5 ppbs VOC2, down to 0.42 when exposed to 150 ppbs of the same VOC. In addition, the $\Delta\mu_{h,norm}$ response on exposure to 5 ppb VOC2 (=0.6) decreased to 0.23 when S1 was exposed to 150 ppbs VOC2. In the case of VOC3, only $\Delta I_{ds,norm}$ @ V_{gs} = 0 could differentiate between the different concentrations (changed from 0.36 on exposure to 5 ppb up to 2.1 on exposure to 150 ppb VOC3). Increasing the concentration of VOC3 from 150 to 500 ppb resulted in a decrease in the normalized response of the current, indicating a change in the mechanism of the response. When examining the response of the various features to VOC4 and VOC5, it can easily be seen that the lower concentrations cannot be distinguished, and the only concentration which can be identified is the highest concentration (500 ppb), which is much higher than the variations in the concentration of these compounds in the breath. Possible mechanisms that might explain these changes are found in SI, section 3.

To demonstrate the high performance of S1, we have plotted the representative FET features (V_{th}, μ_h, and I_{ds} @ V_{gs} = 0) of and S1−S7, on exposure to the various concentrations of VOC1 to VOC5, on a hot plot (Figure 3). When comparing the response of S1 to the responses of the other sensors, we see that the remaining sensors have similar responses to both the potential gastric cancer VOCs and the confounding VOCs (S3 and S5) or respond more strongly to the confounding factors (S2, S4, and S6). In few instances, such as in selected features of S7, the sensors have negligible responses to all VOCs. Figure S1 in SI presents the sensing responses of S2 on exposure to the VOCs listed in Table 2. As seen in the figure, S2 is not very responsive to VOC1. Rather, the response in this case is within the experimental error. Furthermore, when inspecting the response of S2 to the remaining potential biomarkers, we can say that V_{th} partially responds to VOC2 and μ_h responds to VOC3 in the concentrations of interest. V_{th} responds to low concentrations of VOC4 and VOC5, and the I_{ds} @ V_{gs} = 0 responds only to VOC4. The behavior noted for S2 (responds only to some of gastric cancer VOCs, and also to the confounding VOCs) leads us to believe it will not be useful in separating between breath samples of gastric cancer patients and control cases. Similar analysis and overall conclusions could be projected on S3−S7 (SI, section 2). The raw data that include the averages and variances of the selected features extracted from S2−S7 on exposure to VOC1 to VOC5 are presented in Figures S1−S6. The original raw data for the relationship between the extracted features from S1−S7 and the concentrations of VOC1−5 are presented in Figures S7−S13 (SI, section 2).

dx.doi.org/10.1021/nl504482t | Nano Lett. XXXX, XXX, XXX−XXX

Table 3. Clinical Characteristics of All Volunteers in the Current Study

group		number of patients	age (year)	gender (male:female)	smoker (Y:N)	*H. pylori* (Y:N)
gastric cancer	Stages I and II	6	50 ± 5	2:4	0:6	6:0
	Stages III and IV	13	60 ± 9	10:3	7:6	7:4 (2 unknown)
	unknown stage	11	65 ± 9	8:3	3:6 (2 unknown)	1:0 (10 unknown)
	total	30	60 ± 10	19:11	9:19 (2 unknown)	14:4 (12 unknown)
control	early intestinal metaplasia	23	56 ± 13	6:17	6:17	18:5
	ulcer	9	58 ± 13	3:6	2:7	2:1 (6 unknown)
	healthy stomach	45	54 ± 18	15:30	6:39	25:18 (2 unknown)
	total	77	55 ± 16	24:53	14:63	45:24 (6 unknown)

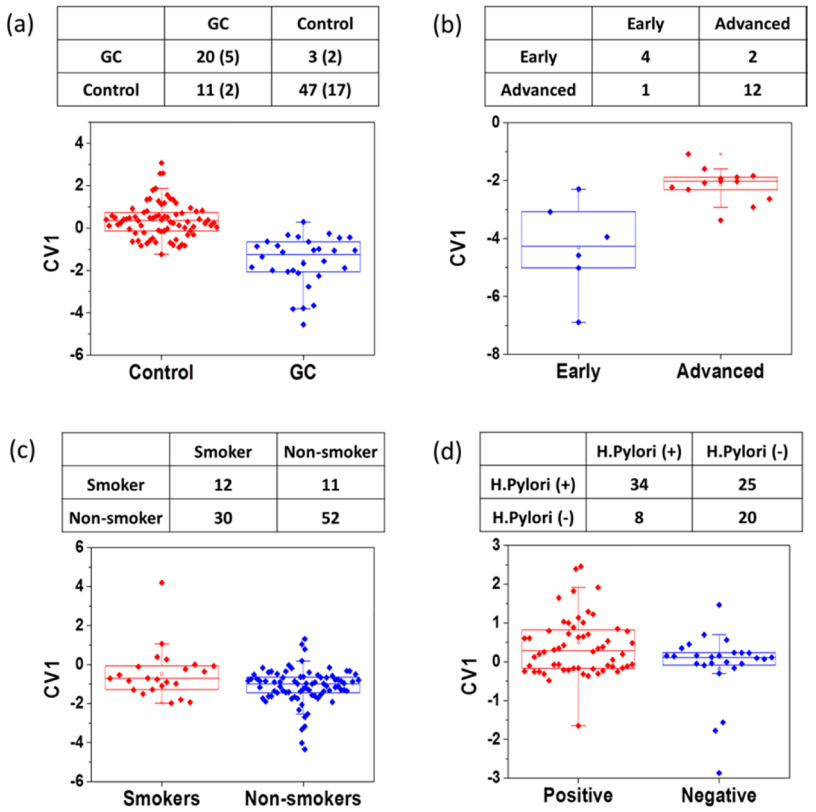

Figure 4. CV1 values and confusion matrices resulting from DFA analysis of the breath samples, performed using S1 features. (a) Gastric cancer vs control. (b) Early stages vs advanced stages. (c) Smokers vs nonsmokers. (d) *H. pylori* positive vs *H. pylori* negative. Values in brackets resulted from blind analysis (test set). DFA is a supervised statistical tool utilized for differentiation between two groups, and CV1 is the most powerful separating dimension, received as output from the DFA analysis.

To validate the applicability of these lab results in real-world conditions, S1 was evaluated for the diagnosis of 30 gastric cancer patients with either early stages (I–II) or advanced stages (III–IV) of the cancer (see details in Table 3) through their collected breath samples. Details on the breath collection process are found in SI, section 1.7. As a reference, breath samples were collected in the same location from 77 volunteers with dyspeptic symptoms but without cancer. So far, these states are considered clinically "healthy" and, therefore, serve as the control group. Detailed information on this category of volunteers is found in Table 3.

Generally speaking, the collected breath samples have been identified with hundreds of different VOCs per individual breath sample, and 214 VOC are present in >85% of the breath samples.[7] Out of the compendium of compounds, only VOC1–VOC3 are linked to gastric cancer conditions. The rest of compounds are considered as confounding clinical and environmental VOCs. Moreover, breath samples are identified with high level of humidity, usually between 80–90% RH— another confounding factor for the anticipated detection process. An additional complication is the effect of smoking and *H. pylori* states on the composition of these VOCs in the body.

All collected breath samples were analyzed by S1 and, for comparison, by S2–S7, as detailed in SI, Section 1.8. Discriminant factor analysis (DFA) was performed on a combination of the three features discussed for the classification of the breath samples collected from gastric cancer patients and control subjects. Briefly, DFA is a supervised statistical analysis method, aiming to find the best possible separation between two previously known groups. The condition applied in the analysis is maximal variance between the two groups, while maintaining minimal variance between members of the same group. The output of the DFA is a set of canonical variables (CVs) which are the dimensions that meet the prior requirement, with CV1 being the dimension with the highest

dx.doi.org/10.1021/nl504482t | *Nano Lett.* XXXX, XXX, XXX–XXX

differentiation power. Various functions can be used in DFA, but in this study we used a linear function for classification. (For more details, please refer to SI, Section 1.8). *To ensure valid results that are free from artifacts or overfitting, we have divided the data set of each analysis as training and validation set. 75% of each group was selected randomly for the training set and* ***25% of each group left out as blind samples.*** Leave-one-out cross-validation was conducted to calculate the classification success in terms of the number of true positive (TP), true negative (TN), false positive (FP), and false negative (FN) predictions.

The interaction between the real breath samples and S1 as well as S2−S7 resulted in rapid and fully reversible changes of the electrical resistance (not shown). Sensing features were extracted from the time-dependent normalized response of each sensor in the area under curve. The net sensing features that were extracted for the breath samples were then divided by the corresponding values that were obtained for the reference calibration compound. The DFA model (see SI, section 1.8) was built based on 75% of the samples to discriminate gastric cancer from the control group. The training set using only one sensor (S1) showed 87% sensitivity, 81% specificity, and 83% accuracy. Plotting the 25% blind samples onto this model achieved 71% sensitivity, 89% specificity, and 85% accuracy (see Figure 3a). The high specificity achieved in the validation set could make the breath test useful for ruling out the test, meaning that a negative result would indicate with high probability the lack of gastric cancer. A critical aspect was considered in this study, in attempting to distinguish the gastric cancer stages (early stages in comparison to advanced stages). A high sensitivity of 92% was achieved for distinguishing the advanced gastric cancer from the early gastric cancer patients. The low specificity of 67% that was achieved in this comparison could be related to the small number of early stage gastric cancer cases (see Figure 3b). Future studies should include a higher number of early stage cases to provide a robust result for distinguishing the early gastric cancer patients. Diagnosis of patients with early stage gastric cancer will help the medical staff take prompt decisions for therapeutic intervention, increasing the overall survival.

To ensure that confounding factors such as smoking and *H. pylori* do not affect our model, the first DFA model was plotted trying to discriminate the smokers from the nonsmokers (**Note:** the majority of subjects were divided into two groups of smokers/nonsmokers, disregarding the subjects whose condition is unknown) showing low accuracy of 60% (see Figure 3c). Sixty-two percent accuracy was achieved when patients with *H. pylori* positive were compared with patients with *H. pylori* negative (see Figure 4d). These results showed that sensor S1 is not affected by the smoking or by the presence of *H. pylori*. The classification achieved by the remaining sensors as well as the classification achieved when using each feature separately can be found in the Supporting Information (see SI, Section 4, Table S1).

In conclusion, we have prepared and fabricated a single sensor that is based on SiNW FET coated with trichloro-(phenethyl)silane (TPS) (S1) that have high detection limited down to 5 ppb. This sensor was able to selectively detect VOCs that are linked with gastric cancer conditions in exhaled breath and to discriminate them from environmental VOCs that exist in exhaled breath samples but do not relate to the gastric cancer per se. The highly selective performance of the TPS-SiNW FET sensor was validated in a real clinical study, using breath samples collected from patients with gastric cancer and from volunteers that have no cancer. Blind analysis validated the ability to use TPS-SiNW FET for simultaneous detection and distinction between gastric cancer and control conditions, irrespective of important confounding factors such as tobacco consumption and gender. Still, this small-scale pilot study does not allow drawing far-reaching conclusions. A multicenter clinical trial with a considerably increased sample size is required to confirm the observed breath prints. We believe the reported SiNW FET sensor can be modified for selective VOC recognition and concentration prediction in other cancer or disease states.

■ ASSOCIATED CONTENT

Ⓢ Supporting Information

Growth of the Si NWs; deposition of the Si NWs array; fabrication of the SiNW FETs; surface modification of the SiNW FETs; surface characterization; sensing experiments upon exposure to VOCs; breath sample collection; breath analysis with the SiNW FET sensors; sensing response of S2−S7 on exposure to VOCs; possible scenarios for sensing the various VOCs by the SiNW FET. This material is available free of charge via the Internet at http://pubs.acs.org.

■ AUTHOR INFORMATION

Corresponding Author

*E-mail (H.H.): hhossam@technion.ac.il.

Notes

The authors declare no competing financial interest.

■ ACKNOWLEDGMENTS

The research leading to these results has received funding from the FP7-Health Program under the LCAOS (grant agreement no. 258868). The sample collection in Latvia was funded in part from the grant no. 305/2012 from Latvian Council of Science. The fabrication was performed at the Micro-Nano Fabrication Unit (MNFU), Technion. The authors thank Mr. Haitham Amal (Technion) for support and assistance.

■ REFERENCES

(1) Burrell, R. A.; McGranahan, N.; Bartek, J.; Swanton, C. *Nature* **2013**, *501*, 338−345.

(2) Murtaza, M.; Dawson, S. J.; Tsui, D. W.; Gale, D.; Forshew, T.; Piskorz, A. M.; Parkinson, C.; Chin, S. F.; Kingsbury, Z.; Wong, A. S.; Marass, F.; Humphray, S.; Hadfield, J.; Bentley, D.; Chin, T. M.; Brenton, J. D.; Caldas, C.; Rosenfeld, N. *Nature* **2013**, *497*, 108−112.

(3) Broza, Y. Y.; Haick, H. *Nanomedicine (Fut. Med.)* **2013**, *8*, 785−806.

(4) Haick, H.; Broza, Y. Y.; Mochalski, P.; Ruzsanyi, V.; Amann, A. *Chem. Soc. Rev.* **2014**, *43*, 1423−1449.

(5) Hakim, M.; Broza, Y. Y.; Barash, O.; Peled, N.; Phillips, M.; Amann, A.; Haick, H. *Chem. Rev.* **2012**, *112*, 5949−5966.

(6) Konvalina, G.; Haick, H. *Acc. Chem. Res.* **2014**, *47*, 66−76.

(7) Xu, Z. q.; Broza, Y. Y.; Ionsecu, R.; Tisch, U.; Ding, L.; Liu, H.; Song, Q.; Pan, Y. Y.; Xiong, F. X.; Gu, K. S.; Sun, G. P.; Chen, Z. D.; Leja, M.; Haick, H. *Br. J. Cancer* **2013**, *108*, 941−950.

(8) Nakhleh, M.; Broza, Y. Y.; Haick, H. *Nanomedicine (Fut. Med.)* **2014**, *9*, 1991−2002.

(9) Barash, O.; Peled, N.; Tisch, U.; Bunn, P. A. J.; Hirsch, F. R.; Haick, H. *Nanomedicine: NBM* **2012**, *8*, 580−589.

(10) Peled, N.; Barash, O.; Tisch, U.; Ionescu, R.; Broza, Y. Y.; Ilouze, M.; Mattei, J.; Bunn, P. A., Jr; Hirsch, F. R.; Haick, H. *Nanomedicine: NBM* **2013**, *9*, 758−766.

(11) Amann, A.; Mochalski, P.; Ruzsanyi, V.; Broza, Y. Y.; Haick, H. *J. Breath Res.* **2014**, *8*, 016003.
(12) Peled, N.; Hakim, M.; Tisch, U.; Bunn, P. A. J. R.; Miller, Y. E.; Kennedy, T. C.; Mattei, J.; Mitchell, J. D.; Weyant, M. J.; Hirsch, F. R.; Haick, H. *J. Thorac. Oncol.* **2012**, *7*, 1528−1533.
(13) Shuster, G.; Gallimidi, Z.; Reiss, A. H.; Dovgolevsky, E.; Billan, S.; Abdah-Bortnyak, R.; Kuten, A.; Engel, A.; Shiban, A.; Tisch, U.; Haick, H. *Breast Cancer Res. Treat.* **2011**, *126*, 791−796.
(14) Bashouti, M. Y.; Stelzner, T.; Berger, A.; Christiansen, S.; Haick, H. *J. Phys. Chem. C* **2008**, *112*, 9168−19172.
(15) Assad, O.; Puniredd, S. R.; Stelzner, T.; Christiansen, S.; Haick, H. *J. Am. Chem. Soc.* **2008**, *130*, 17670−17671.
(16) Bashouti, M. Y.; Stelzner, T.; Berger, A.; Christiansen, S.; Haick, H. *J. Phys. Chem. C* **2009**, *113*, 14823−14828.
(17) Bashouti, M. Y.; Tung, R. T.; Haick, H. *Small* **2009**, *5*, 2761−2769.
(18) Ermanok, R.; Assad, O.; Zigelboim, K.; Wang, B.; Haick, H. *ACS Appl. Mater. Interface* **2013**, *5*, 11172−11183.
(19) Paska, Y.; Stelzner, T.; Christiansen, S.; Haick, H. *ACS Nano* **2011**, *5*, 5620−5626.
(20) Paska, Y.; Haick, H. *ACS Appl. Mater. Interface* **2012**, *4*, 2604−2617.
(21) Paska, Y.; Stelzner, T.; Assad, O.; Tisch, U.; Christiansen, S.; Haick, H. *ACS Nano* **2012**, *6*, 335−345.
(22) Bashouti, M. Y.; Sardashti, K.; Schmitt, S. W.; Pietsch, M.; Ristein, J.; Haick, H.; Christiansen, S. H. *Prog. Surf. Sci.* **2013**, *88*, 39−60.
(23) Patolsky, F.; Zheng, G. F.; Lieber, C. M. *Anal. Chem.* **2006**, *78*, 4260−4269.
(24) Cui, Y.; Wei, Q. Q.; Park, H. K.; Lieber, C. M. *Science* **2001**, *293*, 1289−1292.
(25) Wang, W. U.; Chen, C.; Lin, K.-H.; Fang, Y.; Lieber, C. M. *Proc. Natl. Acad. Sci. U.S.A.* **2005**, *102*, 3208−3212.
(26) McAlpine, M. C.; Agnew, H. D.; Rohde, R. D.; Blanco, M.; Ahmad, H.; Stuparu, A. D.; Goddard, W. A.; Heath, J. R. *J. Am. Chem. Soc.* **2008**, *130*, 9583−9589.
(27) Yanga, Z.; Huangb, Y.; Chena, G.; Guoc, Z.; Chengb, S.; Huange, S. *Sens. Actuators B* **2009**, *140*, 549−556.
(28) Zhou, X. T.; Hu, J. Q.; Li, C. P.; Ma, D. D. D.; Lee, C. S.; Lee, S. T. *Chem. Phys. Lett.* **2003**, *369*, 220−224.
(29) Röck, F.; Barsan, N.; Weimar, U. *Chem. Rev.* **2008**, *108*, 705−725.
(30) Wang, B.; Cancilla, J. C.; Torrecilla, J.; Haick, H. *Nano Lett.* **2014**, *14*, 933−938.
(31) Wang, B.; Haick, H. *ACS Appl. Mater. Interfaces* **2013**, *5*, 2289−2299.
(32) Wang, B.; Haick, H. *ACS Appl. Mater. Interfaces* **2013**, *5*, 5748−5756.